

1       **Identification of bis-benzylisoquinoline alkaloids as SARS-CoV-2 entry**

2                   **inhibitors from a library of natural products in vitro**

3       **Running title:** SARS-CoV-2 entry inhibitors

4       Chang-Long He<sup>1, #</sup>, Lu-Yi Huang<sup>1, #</sup>, Kai Wang<sup>1, #</sup>, Chen-Jian Gu<sup>2</sup>, Jie Hu<sup>1</sup>, Gui-Ji

5       Zhang<sup>1</sup>, Wei Xu<sup>2</sup>, You-Hua Xie<sup>2, 3,\*</sup>, Ni Tang<sup>1,\*</sup>, Ai-Long Huang<sup>1,\*</sup>

6       <sup>1</sup>Key Laboratory of Molecular Biology for Infectious Diseases (Ministry of  
7       Education), Institute for Viral Hepatitis, Department of Infectious Diseases, The  
8       Second Affiliated Hospital, Chongqing Medical University, Chongqing, 400010,  
9       China

10      <sup>2</sup>Key Laboratory of Medical Molecular Virology (MOE/NHC/CAMS), Department of  
11      Medical Microbiology and Parasitology, School of Basic Medical Sciences, Shanghai  
12      Medical College, Fudan University, Shanghai, 201102, China.

13      <sup>3</sup>Children's Hospital, Fudan University, Shanghai, 201102, China.

14      <sup>#</sup>These authors contributed equally to this work.

15      **\*Corresponding authors:**

16      **Ai-Long Huang, Ni Tang**, Key Laboratory of Molecular Biology for Infectious  
17      Diseases (Ministry of Education), Institute for Viral Hepatitis, Department of  
18      Infectious Diseases, The Second Affiliated Hospital, Chongqing Medical University,  
19      Chongqing, China. Phone: 86-23-68486780, Fax: 86-23-68486780, E-mail:  
20      [ahuang@cqmu.edu.cn](mailto:ahuang@cqmu.edu.cn) (A.L.H.), [nitang@cqmu.edu.cn](mailto:nitang@cqmu.edu.cn) (N.T.); **You-Hua Xie**, Key  
21      Laboratory of Medical Molecular Virology (MOE/NHC/CAMS), School of Basic

22 Medical Sciences, Shanghai Medical College, Fudan University, e-mail,

23 [yhxie@fudan.edu.cn](mailto:yhxie@fudan.edu.cn)

24 **Abstract**

25 Coronavirus disease 2019 (COVID-19) caused by severe acute respiratory syndrome  
26 coronavirus 2 (SARS-CoV-2) is a major public health issue. To screen for antiviral  
27 drugs for COVID-19 treatment, we constructed a SARS-CoV-2 spike (S) pseudovirus  
28 system using an HIV-1-based lentiviral vector with a luciferase reporter gene to  
29 screen 188 small potential antiviral compounds. Using this system, we identified nine  
30 compounds, specifically, bis-benzylisoquinoline alkaloids, that potently inhibited  
31 SARS-CoV-2 pseudovirus entry, with EC<sub>50</sub> values of 0.1–10 μM. Mechanistic studies  
32 showed that these compounds, reported as calcium channel blockers (CCBs),  
33 inhibited Ca<sup>2+</sup>-mediated membrane fusion and consequently suppressed coronavirus  
34 entry. These candidate drugs showed broad-spectrum efficacy against the entry of  
35 several coronavirus pseudotypes (SARS-CoV, MERS-CoV, SARS-CoV-2 [S-D614,  
36 S-G614, N501Y.V1 and N501Y.V2]) in different cell lines (293T, Calu-3, and A549).  
37 Antiviral tests using native SARS-CoV-2 in Vero E6 cells confirmed that four of the  
38 drugs (SC9/cepharanthine, SC161/hernandezine, SC171, and SC185/neferine)  
39 reduced cytopathic effect and supernatant viral RNA load. Among them,  
40 cepharanthine showed the strongest anti-SARS-CoV-2 activity. Collectively, this  
41 study offers new lead compounds for coronavirus antiviral drug discovery.  
42

43 **Introduction**

44       Coronavirus disease 2019 (COVID-19) caused by severe acute respiratory  
45       syndrome coronavirus 2 (SARS-CoV-2) is a major public health issue. The spike (S)  
46       protein mutation D614G (a single change in the genetic code; D = aspartic acid, G =  
47       glycine) became dominant in SARS-CoV-2 during global pandemic, which displayed  
48       increased infectivity.<sup>1</sup> Entry of a virus into host cells is one of the most critical steps  
49       in the viral life cycle. Since blockade of the entry process is a promising therapeutic  
50       option for COVID-19, research attention has been focused on the discovery of viral  
51       entry inhibitors. Although SARS-CoV-2 entry inhibitor development is very attractive,  
52       no candidates have progressed into clinical trials yet.

53

54

55 **Materials and Methods**

56 **Plasmids**

57 The codon-optimized gene encoding SARS-CoV-2 spike (S) protein (GenBank:  
58 QHD43416) with 19 amino acids deletion at the C-terminal was synthesized by Sino  
59 Biological Inc (Beijing, China), and cloned it into the pCMV3 vector between the  
60 restriction enzyme *Kpn*I and *Xba*I sites (denoted as pS-D614). The recombinant  
61 plasmid pS-D614 was used as template, and the D614G mutant S-expressing plasmid  
62 (denoted as pS-G614) was constructed by site-directed mutagenesis. N501Y.V1  
63 (Variant 1) mutant Spike proteins of SARS-CoV-2 were codon-optimized and  
64 synthesized by GenScript Inc (Nanjing, China) and cloned into pCMV3 vector  
65 (denoted as pS-Variant1). N501Y.V2 (Variant 2) mutant Spike-expressing plasmid  
66 (denoted as pS-Variant2) was constructed by site-directed mutagenesis, with pS-D614  
67 plasmid as a template. SARS-CoV S-expressing plasmid (Cat: VG40150-ACGLN,  
68 named as pS-SARS) and MERS-CoV S-expressing plasmid (Cat: VG40069-CF,  
69 named as pS-MERS) were obtained from Sino Biological Inc (Beijing, China). The  
70 VSV-G-expressing plasmid pMD2.G was donated by Prof. Ding Xue from Tsinghua  
71 University (Beijing, China). The HIV-1 NL4-3  $\Delta$ Env Vpr luciferase reporter vector  
72 (pNL4-3.Luc.R-E-) constructed by N. Landau was donated by Prof. Cheguo Cai from  
73 Wuhan University (Wuhan, China). Human ACE2 and DPP4 expression plasmids  
74 were derived from GeneCopoeia (Guangzhou, China).

75

76 **Cell lines and cell culture**

77 HEK 293T, A549, and Calu3 cells were purchased from the American Type Culture  
78 Collection (ATCC, Manassas, VA, USA). Cells were cultured at 37 °C and 5% CO<sub>2</sub>  
79 atmosphere in Dulbecco's modified Eagle medium (DMEM; Hyclone, Waltham, MA,  
80 USA) containing 10% fetal bovine serum (FBS; Gibco, Rockville, MD, USA), 100  
81 mg/mL of streptomycin, and 100 units/mL of penicillin. HEK 293T cells transfected  
82 with human ACE2 and DPP4 (293T-ACE2, 293T-DPP4) were cultured under the  
83 same conditions with the addition of G418 (0.5 mg/mL) to the medium.

84

#### 85 **Antigens and antibodies**

86 The RBD domain of SARS-CoV-2 S protein (His-tag) were synthesized by Prof.  
87 Xuefei Cai at Key Laboratory of Molecular Biology for Infectious Diseases (Ministry  
88 of Education), Chongqing Medical University. The anti-RBD monoclonal antibody  
89 was kindly provided by Prof. Aishun Jin from Chongqing Medical University.  
90 RBD-binding peptide SBP1 derived from human ACE2 α helix 1  
91 (Ac-IEEQAKTFLDKFNHEAEDLFYQS-NH<sub>2</sub>) was synthesized by GenScript  
92 (Nanjing, China).

93

#### 94 **Compounds and reagents**

95 Custom compound library containing 188 small molecules, remdesivir, and aloxistatin  
96 (E-64d) were purchased from MedChemExpress (HY-L027) and Chemdiv.  
97 BAPTA-AM (T6245) was purchased from TargetMol. All the compounds were  
98 dissolved in dimethyl sulfoxide (DMSO) at a stock concentration of 20 mM.

99

100 **Cell cytotoxicity assay**

101 The CellTiter 96® AQueous One Solution Cell Proliferation Assay (G3582, Promega,  
102 USA) was used to assess cell viability according to the product's description. Briefly,  
103 HEK 293T cells were dispensed into 96-well plate ( $2 \times 10^4$  cells/well), cultured in  
104 medium containing gradient concentrations of the compound for 72 hours at 37 °C in  
105 a humidified 5% CO<sub>2</sub> incubator. The cells were incubated with 100 µl fresh medium  
106 after removal of the medium. Then 20 µl of CellTiter 96® AQueous One Solution  
107 Reagent was added into each sample well and incubating the plate was incubated at  
108 37°C for 1-4 hours in a humidified 5% CO<sub>2</sub> atmosphere. The absorbance at 490 nm  
109 was measured using a microplate reader (Synergy H1, BioTek, USA).

110

111 **Pseudovirus production and quantification**

112  $5 \times 10^6$  HEK 293T cells were co-transfected with 6 µg each of pNL4-3.Luc.R-E- and  
113 recombinant plasmid (pS-SARS, pS-MERS, pS-D614, pS-G614, pS-Variant1, or  
114 pS-Variant2) using Lipofectamine 3000 Transfection Reagent (Invitrogen, Rockville,  
115 MD) according to the manufacturer's instructions. After 48 h transfection,  
116 pseudotyped viruses expressing S-SARS, S-MERS, S-D614, S-G614, N501Y.V1, and  
117 N501Y.V2 spike protein were harvested, centrifuged and filtered through 0.45 µm  
118 filters, and subsequently stored at -80°C. 293T cells were co-transfected with  
119 pNL4-3.Luc.R-E- and pMD2.G plasmid to collect the VSV-G pseudovirus.

120 The copies of the pseudovirus were expressed as numbers of viral RNA genomes  
121 per mL of viral stock solution and determined using RT-qPCR with primers and a  
122 probe that targeting LTR. Sense primer: 5'-TGTGTGCCGTCTGTTGTGT-3',  
123 anti-sense primer: 5'-GAGTCCTGCGTCGAGAGAGC-3', probe:  
124 5'-FAM-CAGTGGCGCCCGAACAGGGA-BHQ1-3'. Briefly, viral RNAs were  
125 extracted according to the manufacturer's instructions with TRIzol reagent  
126 (Invitrogen). Then, the TaqMan One-Step RT-PCR Master Mix Reagents (Applied  
127 Biosystems, Thermo Fisher) was used to amplify total RNAs. pNL4-3.Luc.R-E-  
128 vector with certain copies was used to generate standard curves. All the pseudotyped  
129 viruses were titrated to the uniform titer (copies/mL) for the following research.

130

### 131 **Compound screening**

132 For pseudovirus-based inhibition assay, 188 compounds were screened via luciferase  
133 activity. HEK 293T cells cultured in 96-well plate ( $2 \times 10^4$  cells/well) were incubated  
134 with each compound (20  $\mu$ M) for 1 hour and were infected with the same amount of  
135 pseudovirus ( $3.8 \times 10^4$  copies in 50  $\mu$ L). The cells were replaced to fresh DMEM  
136 medium 8 h post-infection. Cells were lysed by 30  $\mu$ l lysis buffer (Promega, Madison,  
137 WI, USA) at 72 h post-infection to measure RLU with luciferase assay reagent  
138 (Promega, Madison, WI, USA) according to the product description. All data were  
139 performed at least three times and expressed as means  $\pm$  standard deviations (SDs).

140

### 141 **Cell-cell fusion assay**

142 HEK 293T effector cells were transfected with plasmid pAdTrack-T04-GFP  
143 encoding green fluorescent protein (GFP) or pS-G614 encoding the corresponding  
144 SARS-CoV-2 S protein. 293T-ACE2 cells were used as target cells. At 8 h  
145 post-transfection, the effector cells were washed twice with PBS and were pretreated  
146 with compounds or DMSO as control for another 16h. Subsequently, the effector cells  
147 were overlaid on target cells at a ratio of approximately one S-expressing cell to two  
148 receptor-expressing cells with about 90% confluent. After a 4-hour coculture, images  
149 of syncytia were captured with an inverted fluorescence microscope (Nikon eclipse  
150 Ti, Melville, NY).

151 For quantification of cell-cell fusion, three fields were randomly selected in each  
152 well to count the fused and unfused cells. The fused cells were at least twice as large  
153 as the unfused cells, and the fluorescence intensity was weaker in fused cells since  
154 GFP diffusion from one effector cell to target cells. The percentage of cell-cell fusion  
155 was calculated as: [(number of the fused cells/number of the total cells)  $\times$  100%].

156

157 **Competitive ELISA**

158 The recombinant RBD proteins derived from SARS-CoV-2 were coated on 96-well  
159 microtiter plate (50ng/well) at 4°C overnight. After blocked with blocking buffer (5%  
160 FBS and 2% BSA in PBS) for 1 hour at 37°C, serial dilution solutions of compounds,  
161 ACE2 peptide SBP1 or DMSO were added into the plates and incubated at 37°C for 1  
162 hour. Plates were washed five times with phosphate-buffered saline, 0.05% Tween-20  
163 (PBST) to remove the free drug or DMSO. The wells were incubated with mouse

164 anti-RBD monoclonal antibody (1:1000 dilution) for 1 hour at 37°C, and then washed  
165 with PBST five times and incubated with Horseradish peroxidase (HRP)-conjugated  
166 goat anti-mouse antibody (Abmart, Shanghai, China) for 1 hour at 37°C. TMB  
167 substrate was added and incubated for 15 minutes at 37°C for color development,  
168 finally the absorbance at 450 nm was measured by a microplate reader.

169

170 **Differential scanning fluorimetry**

171 Briefly, purified His-RBD was diluted to 200 µg/mL in PBS buffer containing Sypro  
172 Orange 5× (ThermoFisher) in a 96-well white PCR plate. Compounds and ACE2  
173 derived peptide SBP1 were added at a final concentration of 20 µM. All samples were  
174 tested in triplicate with a Bio-Rad RT-PCR system. The samples were first  
175 equilibrated at 25 °C for 3 min, then heated from 25 °C to 85 °C with a step of 1 °C  
176 per 1 min, and the fluorescence signals were continuously collected using CFX  
177 Maestro.

178

179 **Functional analysis of Ca<sup>2+</sup> in pseudovirus infectivity**

180 293T-ACE2 cells were seeded in 96-well plate (2x10<sup>4</sup> cells/well) and incubated at 37  
181 °C for 8h. For extracellular calcium depletion assays, cells were washed three times  
182 using PBS with or without Ca<sup>2+</sup>. Calcium-free medium with or without 2 mM calcium  
183 chloride and 5 µM compounds were added and incubated for 1h at 37°C. Next,  
184 S-G614 pseudovirus was added to the cells for 8 h at 37°C. For intracellular calcium  
185 depletion assays, cells were washed three times using PBS with or without Ca<sup>2+</sup>,

186 DMEM with BAPTA-AM (20  $\mu$ M) or DMSO and gradient concentrations of  
187 compounds were added and incubated for 2 h at 37°C. In the following, S-G614  
188 pseudovirus was added to infect the cells for 8 h at 37°C. For both types of assays,  
189 complete medium was then added after removed the medium. The cells were  
190 measured by luciferase activity.

191

192 **Cellular cholesterol measurement**

193 Cellular cholesterol was measured using the Cholesterol/Cholesterol Ester-Glo<sup>TM</sup>  
194 Assay (J3190, Promega, USA) according to the product's description. In short, HEK  
195 293T-ACE2 cells were assigned to 96-well plates ( $4 \times 10^4$  cells/well) and cultured for  
196 24 hours at 37 °C with 5  $\mu$ M compounds. DMSO was used as negative control. The  
197 medium in the 96-well plate was removed and cells was washed twice with 200  $\mu$ l  
198 PBS. Then, 50  $\mu$ l of cholesterol lysis solution was added, shaking the plate carefully  
199 and incubating for 30 minutes at 37°C. Following, 50  $\mu$ l of cholesterol detection  
200 reagent was added with esterase or without esterase to all wells and the plate was  
201 incubated at room temperature for 1 hour. Finally, recording luminescence with a  
202 plate-reading luminometer. Total cholesterol concentration was calculated by  
203 comparing the luminescence of samples and controls under the same condition.

204

205 **Cytopathic effect (CPE) assay and quantification of SARS-CoV-2 infection**

206 Vero E6 cells were dispensed into 96-well plate ( $4.0 \times 10^4$  cells/well), pre-treated with  
207 medium containing compounds or DMSO for 1 hour at 37 °C. Then 60  $\mu$ l DMEM

208 medium which supplemented with compounds or DMSO was replaced immediately,  
209 the same amount of SARS-CoV-2 (100 TCID<sub>50</sub>/well) was added and incubated for 1  
210 hour at 37 °C. The mixture was removed and the cells were washed twice with PBS,  
211 and cultured with 100 µl fresh medium for 48 hours at 37 °C with 5% CO<sub>2</sub>  
212 atmosphere. Cytopathic effects (CPE) induced by the virus was observed using  
213 microscope at 48 h post-inoculation. Cell culture supernatant was collected at 48 h  
214 post-infection for viral RNA quantification using the novel coronavirus real-time  
215 RT-PCR Kit (Shanghai ZJ Bio-Tech Co, Ltd, Shanghai, China). Remdesivir (5 µM)  
216 was used as positive control in the experiment.

217

218 **Statistical analyses**

219 Data were analyzed using GraphPad Prism version 6.0 software and were presented as  
220 means ± SD. Statistical significance was determined using ANOVA for multiple  
221 comparisons. Student's t test was applied to compare the two groups. Differences with  
222 P values < 0.05 were deemed statistically significant.

223

224 **Results**

225 Using a luciferase-expressing pseudovirus encoding SARS-CoV-2 S (G614)  
226 protein, a library of 188 natural compounds ([Supplementary Tab. S1](#)) was screened in  
227 293T-ACE2 cells (HEK 293T cells overexpressing human angiotensin-converting  
228 enzyme 2) to find novel anti-SARS-CoV-2 entry inhibitors. A workflow chart of  
229 screening is shown in [Fig. 1a](#). After a preliminary screening, 41 compounds  
230 associated with a relative infection rate <30% ([Fig. 1b](#)) were identified. We selected  
231 19 compounds with low cytotoxicity for further testing ([Supplementary Tab. S2](#), [Fig.](#)  
232 [S1](#)). Among the 19 hits, nine compounds (SC9, SC161, SC171, SC182–187) with  
233 relatively high activity ( $EC_{50} < 10 \mu M$ ), low cytotoxicity ( $CC_{50} > 20 \mu M$ ), and high  
234 specificity ( $SI > 10$ ) were selected for subsequent analyses. Specifically, all these  
235 compounds were bis-benzylisoquinoline alkaloids except SC171.

236 Next, we analyzed the relationship between the antiviral efficacy of the nine  
237 selected compounds against S-G614 pseudovirus and the timing of treatment  
238 ([Supplementary Fig. S2](#)). We divided the S-G614 pseudovirus entry into three stages:  
239 pretreatment, pseudovirus entry, and pseudovirus post-entry. In total, eight  
240 experimental groups were set up for each compound, including seven treatment  
241 groups (A–G) and a control group. Importantly, pretreatment with each compound  
242 ([group B](#)) significantly inhibited S-G614 pseudovirus infection. In the pseudovirus  
243 entry stage ([group C](#)), the compounds exerted similar suppressive effects. However, in  
244 the pseudovirus post-entry stage ([group D](#)), none of the compounds showed any  
245 inhibitory effect. Our data demonstrated that the nine selected compounds showed

246 effective entry blockade presenting in the pretreatment stage, indicating that they  
247 target host factors at the entry stage.

248 Cell lines mimicking important aspects of respiratory epithelial cells should be  
249 used when analyzing the anti-SARS-CoV-2 activity. Hence, we determined their EC<sub>50</sub>  
250 values against S-G614 pseudovirus in Calu-3 and A549 cells ([Supplementary Fig.](#)  
251 [S3a-i](#)). Five compounds (SC9, SC161, SC171, SC182, and SC185) with EC<sub>50</sub> < 10  
252 μM in all three cells lines were selected for subsequent experiments.

253 To determine whether these compounds have broad-spectrum antiviral effects  
254 against coronaviruses, we constructed S-D614, N501Y.V1 (B.1.1.7), N501Y.V2 (B.  
255 1.351), S-SARS, and S-MERS pseudoviruses using the same lentiviral system as  
256 S-G614, and then determined the EC<sub>50</sub> values of SC9 (cepharanthine, [Fig. 1c](#)), SC161  
257 (hernandezine, [Fig. 1d](#)), SC171 ([Fig. 1e](#)), SC182 (tetrandrine, [Fig. 1f](#)), and SC185  
258 (neferine, [Fig. 1g](#)) against these pseudoviruses in 293T cells expressing ACE2 or  
259 dipeptidyl peptidase 4 (DPP4). Interestingly, SC9, SC161, SC171, and SC185  
260 exhibited highly potent pan-inhibitory activity against S-pseudotyped coronaviruses  
261 including two emerging SARS-CoV-2 variants N501Y.V1 and N501Y.V2, reported in  
262 United Kingdom and South Africa ([Supplementary Fig. S3j](#)). As SARS-CoV and  
263 SARS-CoV-2 have been reported to enter host cells via binding to ACE2, and while  
264 DPP4 is critical for MERS-CoV entry, it could be ruled out that the five compounds  
265 interfere with ACE2 to block pseudovirus entry.

266 Then, we used competitive ELISAs and thermal shift assays to determine  
267 whether these five compounds interact with the receptor-binding domain (RBD) in S

268 protein of SARS-CoV-2. SBP1, a peptide derived from the ACE2  $\alpha$ 1 helix, bound  
269 RBD of SARS-CoV-2 and exhibited a weak ability to inhibit the entry of S-G614  
270 pseudovirus (Supplementary Fig. S4a), whereas the interaction between SC9, SC161,  
271 SC171, or SC185 and RBD was negligible (Supplementary Fig. S4c-d). Thus, the  
272 blockade of virus entry by these candidate compounds is not related to interaction  
273 with the SARS-CoV-2 RBD domain.

274 Following attachment to host receptor, the membrane fusion process mediated by  
275 S protein of SARS-CoV-2 plays an important role in viral entry. Thus, we examined  
276 whether these compounds perturb cell fusion mediated by SARS-CoV-2 S protein.  
277 Compared to DMSO, SC9, SC161, SC182, and SC185 at 5  $\mu$ M potently inhibited  
278 SARS-CoV-2 S-mediated membrane fusion of 293T cells with approximately 90%  
279 decrease of fusion rates (Fig. 1h, Supplementary Fig. S4e). Previous studies have  
280 shown that the calcium ion ( $\text{Ca}^{2+}$ ) plays a critical role in SARS-CoV or MERS-CoV  
281 S-mediated fusion with host cells.<sup>2</sup> Calcium channel blockers (CCBs), originally used  
282 to treat cardiovascular diseases, are supposed to have a high potential to treat  
283 SARS-CoV-2 infections.<sup>3</sup> We noted that the identified bis-benzylisoquinoline  
284 alkaloids had been reported as CCBs.<sup>4</sup> Herein, the bis-benzylisoquinoline CCBs  
285 abolished S-ACE2-mediated membrane fusion in 293T-ACE2 cells. Calcium-free  
286 medium or intracellular  $\text{Ca}^{2+}$  chelation with BAPTA-AM significantly diminished  
287 SARS-CoV-2 pseudovirus infection (Fig. 1i, Supplementary Fig. S4f-i), suggesting  
288 that  $\text{Ca}^{2+}$  is required for SARS-CoV-2 entry. Upon pretreatment with BAPTA-AM, the  
289 bis-benzylisoquinoline CCBs had approximately 10-fold higher  $\text{EC}_{50}$  values than

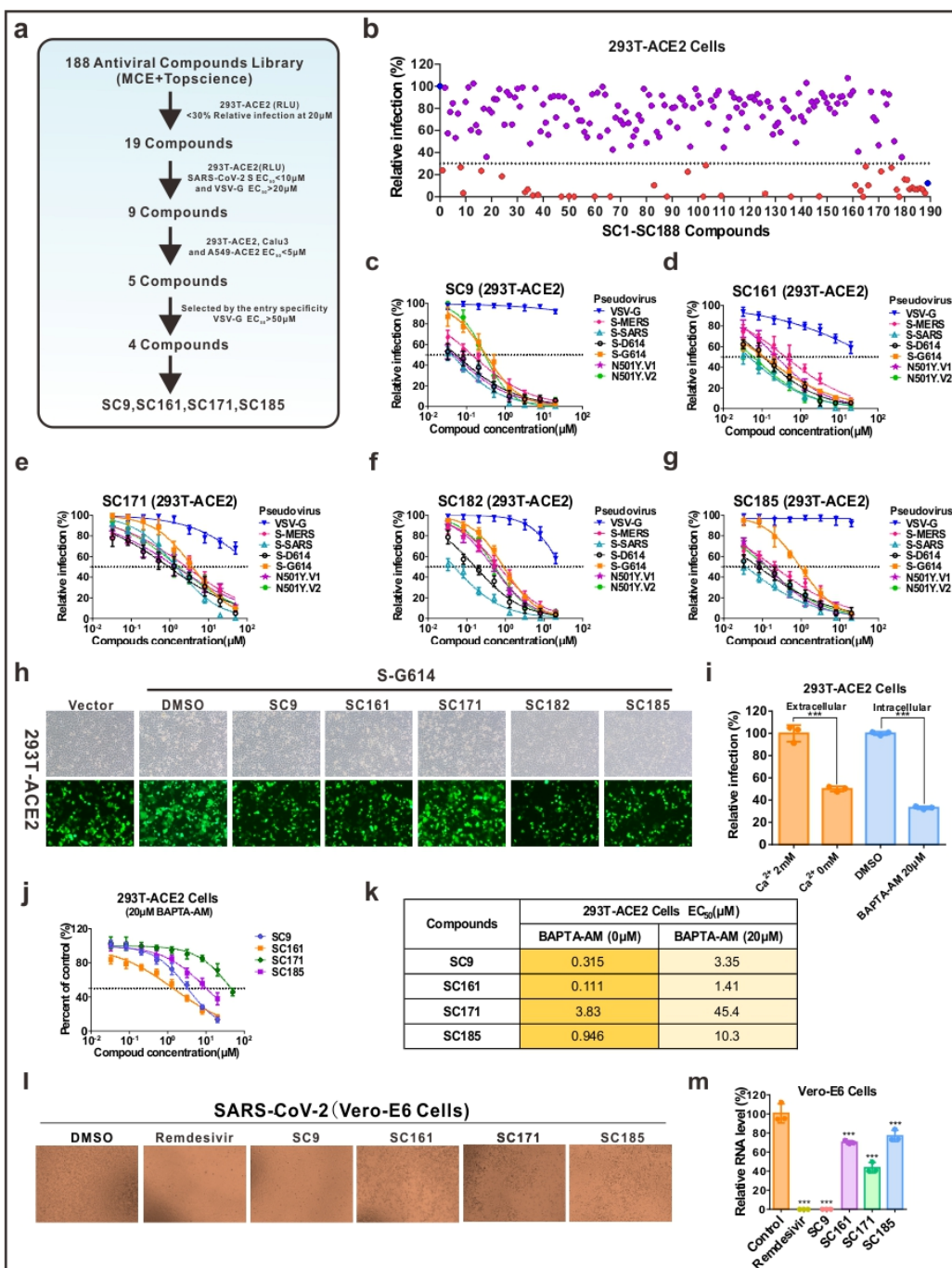
290 those without BAPTA-AM pretreatment (Fig. 1j-k, Supplementary Fig. S4j-k).  
291 Additionally, perturbation of the cholesterol biosynthesis pathway with the CCB  
292 amlodipine reduced viral infection.<sup>5</sup> Consistent herewith, the bis-benzylisoquinoline  
293 CCBs upregulated intracellular cholesterol (Supplementary Fig. S4i), which also  
294 likely contributes to inhibition of viral infection. These data indicated that blockade of  
295 S-G614 pseudovirus entry by bis-benzylisoquinoline CCBs mainly depends on  
296 calcium homeostasis.

297 Finally, the antiviral activities of SC9 (cepharanthine), SC161 (hernandezine),  
298 SC171, and SC185 (neferine) were confirmed in Vero E6 cells infected with native  
299 SARS-CoV-2. SARS-CoV-2 induced cytopathogenic effect (CPE) and the viral RNA  
300 levels were partly inhibited by these compounds, with SC9 (cepharanthine) at the  
301 highest efficacy and the other three compounds much less active. (Fig. 1l-m). The  
302 results showed that these compounds inhibited SARS-CoV-2 to varying degrees and  
303 may be useful as leads for SARS-CoV-2 therapeutic drug development.  
304

305 **Discussion**

306 In summary, we reported a set of bis-benzylisoquinoline alkaloids as coronavirus  
307 entry inhibitors. These inhibitors effectively protected different cell lines (293T,  
308 Calu-3, and A549) from infection by different coronaviruses (SARS-CoV,  
309 MERS-CoV, SARS-CoV-2 [S-D614 and S-G614 variant]) *in vitro*. The compounds  
310 block host calcium channels, thus inhibiting  $\text{Ca}^{2+}$ -mediated fusion and suppressing  
311 virus entry. Considering the effectiveness of CCBs in the control of hypertension, our  
312 study provided clues to support that CCBs may be useful in treating coronavirus  
313 infection in patients with hypertension.

314



315

316 **Fig. 1** Identification of bis-benzylisoquinoline alkaloids as SARS-CoV-2 entry  
 317 inhibitors. **a** Schematic diagram of the screening workflow with selection criteria for  
 318 hits outlined. **b** Scatter plot of primary screening of 188 compounds against S-G614  
 319 infection. Inhibition ratios for all drugs obtained in a preliminary screening are  
 320 represented by scattered points. Red dots indicate the 41 compounds with an

321 inhibition rate  $\geq 70\%$ . DMSO and aloxistatin (blue dot) were used as a negative and  
322 positive control, respectively. **c-g** Dose-response curves of five selected compounds (**c**)  
323 SC9, (**d**) SC161, (**e**) SC171, (**f**) SC182, (**g**) SC185 on VSV-G, S-D614, S-G614,  
324 S-SARS, S-MERS, N501Y.V1, and N501Y.V2 pseudoviruses. **h** Inhibitory effect of  
325 SC9, SC161, SC171, SC182, and SC185 at 5  $\mu\text{M}$  on SARS-CoV-2 S mediated  
326 cell-cell fusion. **i** Effect of extracellular and intracellular  $\text{Ca}^{2+}$  depletion on S-G614  
327 pseudovirus entry in 293T cells. **j-k** Inhibition curves (**j**) and  $\text{EC}_{50}$  values (**k**) of the  
328 compounds against S-G614 pseudovirus entry in the presence of 20  $\mu\text{M}$  BAPTA-AM.  
329 **l** The inhibitory effect of the compounds on native SARS-CoV-2 infection by  
330 observing their cytopathogenic effects. SC9, SC161, SC171, and SC185 were tested  
331 at 10  $\mu\text{M}$ , and DMSO and remdesivir (5  $\mu\text{M}$ ) were used as a negative and positive  
332 control, respectively. **m** The relative viral RNA levels in the SC9, SC161, SC171, and  
333 SC185 (10  $\mu\text{M}$ ) treatment groups were 0.08%, 70.27%, 43.55%, and 76.98%  
334 respectively.  $*P < 0.05$ ;  $**P < 0.01$ ;  $***P < 0.001$ . All experiments were repeated at  
335 least three times.  
336

337 **Acknowledgments**

338 We would like to thank Prof. Cheguo Cai (Wuhan University, Wuhan, China) for  
339 providing the pNL4-3.Luc.R-E- plasmid. This work was supported by the Key  
340 Laboratory of Infectious Diseases, CQMU, 202001, the Science and Technology  
341 Research Program of Chongqing Municipal Education Commission  
342 (KJQN202000418 to L-Y.H.), Emergency Project from the Science & Technology  
343 Commission of Chongqing (cstc2020jscx-fyzx0053, cstc2020jscx-dxwtB0050 to  
344 A-L.H.), and the Emergency Project for Novel Coronavirus Pneumonia from the  
345 Chongqing Medical University (CQMUNCP0302 to K.W.).

346

347 **Author contributions**

348 A.L.H., N.T., and Y.H.X. designed and directed the study. C.L.H., L.Y.H., K.W., J.H.,  
349 and G.J.Z. constructed the pseudoviruses and screened the compounds. C.J.G. and  
350 W.X. performed authentic SARS-CoV-2 assays. All authors reviewed the manuscript  
351 and consented to the description of author contribution.

352

353 **Additional information**

354 The online version of this article contains supplementary material, which is available  
355 to authorized users.

356

357 **Competing interests:** The authors declare no competing interests.

358

359 **References**

360 1 Korber, B. *et al.* Tracking Changes in SARS-CoV-2 Spike: Evidence that  
361 D614G Increases Infectivity of the COVID-19 Virus. *Cell* **182**, 812-827  
362 (2020).

363 2 Tang, T., Bidon, M., Jaimes, J. A., Whittaker, G. R. & Daniel, S. Coronavirus  
364 membrane fusion mechanism offers a potential target for antiviral  
365 development. *Antiviral Res* **178**, 104792 (2020).

366 3 Straus, M. R., Bidon, M., Tang, T., Whittaker, G. R. & Daniel, S. FDA  
367 approved calcium channel blockers inhibit SARS-CoV-2 infectivity in  
368 epithelial lung cells. *Biorxiv* (2020).

369 4 John P. Felix *et al.* Bis(benzylisoquinoline) Analogs of Tetrandrine Block  
370 L-Type Calcium Channels: Evidence for Interaction at the Diltiazem-Binding  
371 Site. *Biochemistry* **31**, 11793-11800 (1992).

372 5 Daniloski, Z. *et al.* Identification of required host factors for SARS-CoV-2  
373 infection in human cells. *Cell* **184**, 1-14 (2020).